Physica Scripta

PAPER

Effects of gallium and arsenic substitution on the electronic and magnetic properties of monolayer SnS

RECEIVED
29 March 2021

REVISED
12 May 2021

ACCEPTED FOR PUBLICATION
20 May 2021

PUBLISHED
31 May 2021

Hamid Ullah[1], **M Waqas Iqbal**[1], **Asad Ali**[2], **N A Noor**[1], **Young-Han Shin**[2], **Muhammad Junaid Iqbal Khan**[3] and **H I El Saeedy**[4]

[1] Department of Physics, RIPHAH University, Campus Lahore, Pakistan
[2] Multiscale Materials Modeling Laboratory, Department of Physics, University of Ulsan, Ulsan 44610, Republic of Korea
[3] Laboratory of Experimental and Theoretical Physics, Department of Physics, Bahauddin Zakariya University, Multan, 60800, Pakistan
[4] Department of Physics—Faculty of Science—King Khalid University, PO Box 9004, Abha, Saudi Arabia

E-mail: hamid.uou@gmail.com **and** hamid.ullah@riphah.edu.pk

Keywords: monolayer SnS, non-transition element, electronic properties, magnetic properties

Abstract

Monolayer tin sulphide (SnS) is an extraordinary two-dimensional material with semiconductor nature. We have explored the doping effects of Gallium (Ga) and Arsenic (As) atoms on the electronic and magnetic properties of monolayer SnS using first-principles calculations. We find that the doped system are energetically stable due to high binding energies. Both the dopants retain the semiconductor nature of monolayer SnS with a tuneable band gap. Interestingly, spin-polarization with magnetic moment of 1.00 μ_B has been induced in both Ga- and As-doped monolayer SnS. Moreover, the realization of magnetic anisotropy energy (MAE) could pave a way to utilize Ga- and As-doped monolayer SnS for applications in magnetic semiconductor devices.

1. Introduction

In 2004 when the graphene was discovered, the material science community has been attracted to graphene-like two-dimensional (2D) material such as silicene, germanene, stanene, phosphorene [1–4]. These 2D materials play a vital role for future electronic applications [5–9]. Similar to group III-V materials [2, 3, 6], there are many materials like group-IV semiconductors (GeS, GeSe. SnS. SnSe) [2, 10–13] which are isoelectronic to that of the black phosphorene [14, 15]. Furthermore, the puckered 2D materials of group VA-VA, such as PN, AsN, SbN and AsP, and examined their performances in metal-oxide-semiconductor field effect transistors (MOSFET) theoretically by Qu *et al* [16]. They found the exceptionally high on-current of 103μA μm^{-1} in the armchair and zigzag directions for AsN and phosphorene, respectively.

Among the already reported 2D materials (graphene, silicine, MoS_2 etc), the mono-layer tin sulfide (SnS), an analogue of phosphorene, has attracted the minds of scientific community due to its fascinating properties [16–18]. For instance, it has been predicted that SnS has absorption coefficient of 10^4 cm^{-1} [19]. Also, an interference effect was observed in SnS at photon energy 25–30 eV [20]. Furthermore, a high carrier concentration (10^{17}–10^{18}) [19], low toxicity and earth abundant [21, 22] properties make it attractive. In comparison to 2D MoS_2, monolayer SnS has a larger electron mobility (7.35 10^4 cm^2 V^1 s^1) [17]. Additionally, ferroelectricity has been realized in monolayer SnS [23, 24]. The 2D SnS also possess huge piezoelectric effect and proved itself to be promising in the field of piezoelectronic and nanosized sensor-devices [25]. Recently, monolayer SnS have been proposed as a selective sensor for NO_2 and successfully operated at room temperature, proving itself to be a new chemiresistors [26]. The nanoflakes of SnS has also been successfully synthesized and reported to be high sensitivity to temperature than graphene and MoS_2 [17]. All of the above studies show the promising nature of SnS nanosheets in the optoelectronic devices. The nontoxic, and earth-abundant nature of SnS with a band gap make it suitable for a number variety of applications in memory switching, optoelectronic devices, and as an anode for rechargeable metal-ion batteries [27–29].

Although monolayer SnS in it pristine form has proven itself with many attractive features and many more other fascinating properties are yet to be investigated. For instance, less attention has been paid to the magnetic properties of doped monolayer SnS with non-transition elements, which is a hurdle in developing the next-generation SnS-based nano-magnetic devices. Pure SnS always exhibit p-type character, and a suitable dopant can make it *n*-type [29, 30]. Several investigations exist in the literature about the doping in SnS to enhance the photovoltaic and optoelectronic properties. For instance, a thin film of Ag-doped SnS has already been prepared to investigate the changes induced by doping in structure, dielectric, and optical properties and showed a significant decrease in the resistivity up to $10^{-3}\,\Omega$ cm with adding impurities [31]. Similarly, the thin-film of Cu@SnS has been pre-pared successfully using the spray pyrolysis method and have observed enhance optoelectronic properties of doped SnS. Also, thin films of Fe@SnS has been fabricated using chemical bath deposition and found that the current density can be controllable via Fe doping in SnS. Recently, the single crystal of SnS doped with Indium (In) and antimony (Sb) has successfully grown using direct vapour transport (DVT) and has confirmed the *p*-type nature of the doped samples [32]. Similarly, Co-/Fe-doped SnS nanoparticles have been synthesized, using precipitation techniques, and revealed that adding the impurities can significantly affect the optical properties, which makes it suitable for the application in optoelectronic devices [32, 33]. Since, these reports paid attention to the photovoltaic and optoelectronic applications of SnS. The spin-polarization could be induced in SnS doped with the non-transition elements that could be fascinating for basic research and technological perspectives. To our knowledge, many experimental investigations exist on the Ga-, and As-doping in SnS where their primary focus on the photovoltaics and optoelectronic properties, and no report is available on the magnetic properties of Ga-/As-doped monolayer SnS.

In this report, we have explored the non-transition element (Ga and As) doping effects on the physical properties of monolayer SnS in terms of electronic and magnetic properties using the first-principles calculations. These atoms belong to group III and group V, which are the neighbour to Sn atom. Additionally, they have an electronic matching configuration, which avoids distortion in the lattice. First, we have investigated the stability of the doped system in terms of binding energies and found that the configurations are energetically favourable. Both the dopants keep the semiconducting nature of monolayer SnS. Interestingly, the dopants induced spin-polarization in monolayer SnS with a computed MAE 0.87 meV, 0.08 meV for Ga- and As-doped monolayer SnS, respectively.

2. Computational details

All the first-principles calculations were carried-out with the spin-polarized density functional theory (DFT) [34]. The generalized gradient approximaztion (GGA) with the Perdew-Burke-Ernzerhoff (PBE) [35, 36] was employed as an exchange-correlation functional with Vienna *ab-initio* Simulation Package (VASP) [37] as a calculator. The supercell ($3 \times 3 \times 1$) approach was adopted to relax the geometry. According to the supercell, the doping concentration was estimated to be 5.88%. To avoid the interaction between neighbouring cells, a vacuum spacing of more than 20 Å was employed in the unit cell. For the Brillouin zone sampling of pristine and doped configurations, the Γ-centered scheme were used with $4 \times 4 \times 1$ *k*-points. The hybrid functional, Heyd-Scuseria-Ernzerhoff (HSE06) [38, 39] was employed to analyze the electronic properties. The spin-polarized DFT is used for the analysis of magnetic properties of the doped configurations. For the analysis of spin interactions (ferromagnetic (FM) and antiferromagnetic (AFM)) between the impurity atoms, we have extended the supercell to $6 \times 3 \times 1$ and replaced two impurity atom at varying distances in the host Sn atoms. To estimate the MAE, a non-collinear spin calculation is employed. The MAE is calculated in terms of the magnetic easy axis and the magnetic hard axis [40, 41]. The total energy method is used for the MAE calculations with $12 \times 12 \times 1$ *k*-points and checked the energy convergence of MAE carefully. Note that the quality of the *k*-mesh should be chosen carefully because of the sensitive nature of MAE to the *k*-mesh [41].

3. Results and discussion

3.1. Structure of Ga-/As-doped monolayer SnS

We have discussed the structural parameters in our previous study [18]. We found in our study [18] that monolayer SnS is layered material with a buckling height of 0.27 Å, as shown in figure 1. The figure 1(a) also shows that the sulphur (S) atom is not exactly on the top of tin (Sn) atom and a slight displacement along the *x*-direction can be seen, which is the origin of ferroelectricity in monolayer SnS [23]. In the last decade, it has been proven that a single transition metal atom (like Co, Pt, and In) can be incorporated into graphene using the pulsed laser deposition techniques [42]. Before moving to calculate other properties, first we have calculated the binding energies, an important entity that shows the binding strength between the dopant atoms and the host monolayer SnS. The binding energy (E_b) for our system is defined as, $E_b = E_{doped} - E_{vacant} - E_{Ga/As}$, where

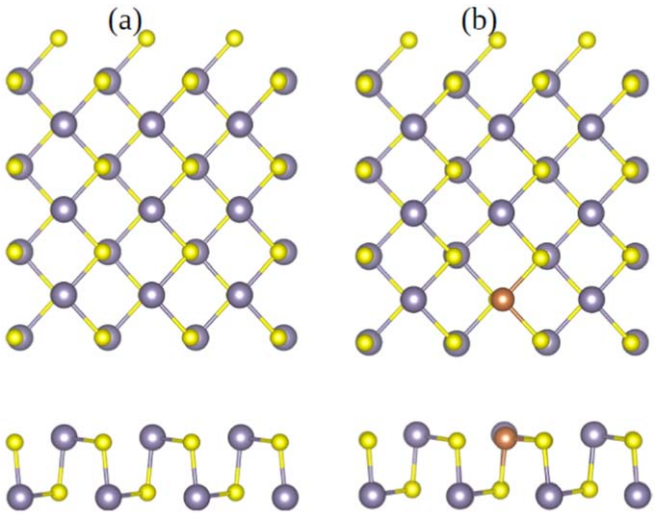

Figure 1. Top/side view of (a) pristine, and (b) Ga-/As-doped monolayer SnS. The grey and yellow color balls represented the Sn and S atoms. The Ga/As atoms are shown with brown color ball in the host supercell.

Table 1. The binding energies (E_b) of the doped systems, Band gaps (E_g) for up (↑) and down (↓) spin channels, minimum distance between the dopant Ga/As and S (d), and the magnetic moments (μ) of single Ga-/As-doped monolayer SnS, and the energy difference (ΔE_i) between the FM and AFM states. The values shown in bracket are the distance between the Ga/As dopant and the upper S atoms layer of the host monolayer SnS.

Dopants		SnS	Ga	As
E_b (eV)		—	5.95	6.90
E_g (eV)	↑	1.89	1.71	2.05
	↓		1.55	1.19
d (Å)		2.57 (2.74)	2.39 (2.49)	2.25 (2.33)
μ (μ_B)		0.00	1.00	1.00
ΔE_i (meV)	ΔE_1	—	−4.34	0.00
	ΔE_2	—	−1.36	0.13
	ΔE_3	—	−0.18	0.44

E_{doped} is the total energy with one Ga-/As-dopant, and E_{vacant} is the energy of one Sn vacancy in the monolayer SnS. The $E_{Ga/As}$ is the total energy of the respective dopant atom. A larger and positive value of the E_b suggesting the energetically favorable nature of the doped configurations.

Furthermore, after confirming the favorable nature of the doped configuration by calculating the E_b, we have noticed a significant penetration of 0.17 Å and 0.06 Å for Ga atom and As atom towards the lower SnS layer. This penetration of the dopants results a decrease in the bond length, which exhibits that the dopant atoms can strongly bind to the host monolayer SnS, as tabulated in table 1. Note that a similar penetration of the dopants was estimated in monolayer SnS doped with transition metals such as Mn, Fe and Co [18].

3.2. Electronic, and magnetic properties

To see the influences of Ga-/As-doping on the electronic properties of monolayer SnS, first, we have investigated the electronic properties of the pristine monolayer SnS, as shown in figure 2. Our results show a semiconductor nature with a band gap of 1.89 eV. From the figure 2, it is obevious that the location of valence band maximum (VBM) lies between Γ and X points and the conduction band minima (CBM) lies between ϒ and Γ points exhibiting that the monolayer SnS is an indirect band gap material. Additionally, we take into account the spin-polarized calculation and found no traces of magnetic ground states in the pristine monolayer SnS. Our calculated results agreeing well with the other experimental and theoretical studies [18, 43]. Note that we have used non-spin polarized band structure for pristine case and spin-polarized one for the doped configurations.

According to the Sn atom electronic configuration ($4d^{10}5s^25p^2$), the two $5p^2$ electrons joined by bonding, and the lone pair is formed by two $5s^2$ electrons [22]. Thus, adding impurities to monolayer SnS can be significantly tuned its electronic properties (decreasing the band gap). Similar trend has also been observed in Ga-doped MoS_2 [44] and Ga-/As-@Germanane monolayer [45]. Note that the dopants Ga/As atoms are

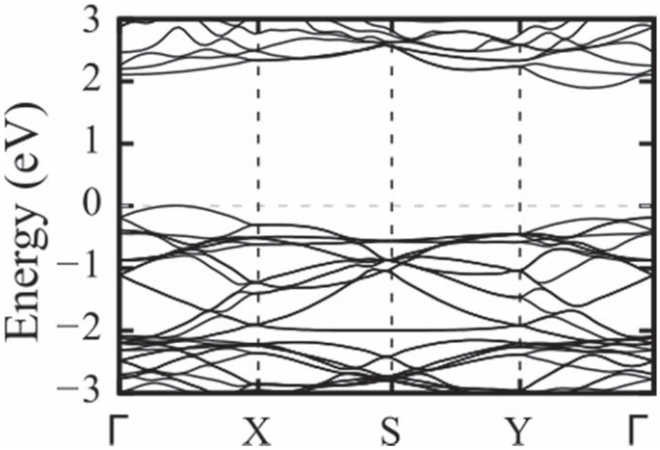

Figure 2. The calculated band structure (BS) of 2D monolayer SnS. The grey dashed lines show the Fermi level.

neighbor to Sn atom which may prevent the lattice distortion in doped configuration. The defects state appears above/below the valence/conduction band in the Ga-/As-doped monolayer SnS.

The spin-polarized BS and density of states (DOS) of the doped configurations are shown in figure 3. In figures 3(a)–(f), one can see that the defects state above/below the valence/conduction band for spin up/down channels of the doped configurations. The defects states do not cross the Fermi-level, and thus both the Ga and As dopant retain the semiconductor property of SnS with band gap values of 1.71 eV and 2.05 eV, respectively. Both Ga and As dopant significantly alters the band gap, see table 1, and figure 3. From table 1, one can observe that the bond length is small between As and S, as compared to Ga and S in the doped configurations. It suggests that the As atom is strongly bound to the S atom, and hence a higher energy is needed for breaking the bond, resulting in a higher band gap of the As-doped monolayer SnS. Similarly, Ga dopant has a large bond length with the neighbor S atoms, which might be loosely bound and required lesser energy to breaking the bonding between them, leading to a decrease the band gap. Thus, a smaller bond length corresponding to a higher band gap. In the doped system, this decrease or increase in the band gap can also be elaborated by bond strength and can be estimated by the electronegativity difference of the host material and the dopant atoms. For example, the electronegativity of Sn, Ga, and As are 1.96, 1.81, and 2.18 respectively, on the Pauling's scale. The Ga dopant has close electronegativity to Sn with a small difference. The other dopant (As) has a larger difference in the electronegativity and a strong binding would expect from it with the host materials. Thus, the doped configuration containing an As atom has larger band gap than the Ga-doped monolayer SnS. We have also calculated the DOS of the Ga- and As-doped monolayer SnS to understand the atomic contribution to the electronic properties and the mechanism of magnetic nature, as shown in figure 3. It can be noted from the figure 3, that doping of Ga and As can induce asymmetric DOS for both states i.e. spin-up and spin-down, exhibiting that the doped SnS is semiconducting with magnetic character. To further understand the mechanism of the magnetic behavior of the doped configuration, we have calculated the project DOS (PDOS), as shown in figure 3.

The Sn-*sp*, S-*p* and Ga-/As-*sp* play a vital role to form the valence band maximum (VBM) and conduction band minimum (CBM), and hence the main contributor to the total DOS as shown in figures 3(c) and (d). The calculated PDOS of both Ga- and As-doped monolayer SnS show that the Sn-*sp*, S-*p* and Ga-/As-*sp* mainly contributed to the total DOS as shown in figures 3(c) and (d).

The DOS results exhibit that magnetic states mainly originate from the *sp*-orbitals and a smaller contribution comes from the S atoms near to the dopant atoms and is confirmed by the spin-density differences as seen in figure 4. We observed that both the dopants keep the semiconductor nature, though a reduction in the band gaps is observed relative to the pure monolayer SnS. We expect that our studied configurations could be promising in spintronics- like spin-polarized communications and memory storage [46–48].

More importantly, the DOS of both the dopants show a clear asymmetry near the Fermi energy, suggesting the possibility of inducing spin polarization in monolayer SnS. For instance, both Ga and As induced spin-polarized ground states with 1.00 μ_B magnetic moment. Our calculated magnetic moment for Ga and As doped in SnS monolayer are in the range of Co-doped MoS_2 monolayer [49] and nonmetal atoms doped in GaS monolayers [50]. Isolated Ga ($4s^2 4p^1$) and As ($4s^2 4p^3$) atoms have one less and one additional valence electrons than Sn ($5s^2 5p^2$) atom, respectively, which clarifies the spin-polarization in Ga- and As-doped SnS. We compared the calculated results with other 2D materials doped with impurities such as 3*d* element-MoS_2 [51] and 4*d* elements-SnS_2 [48, 52] and found the same trend. Additionally, in our previous work [18] the doping of

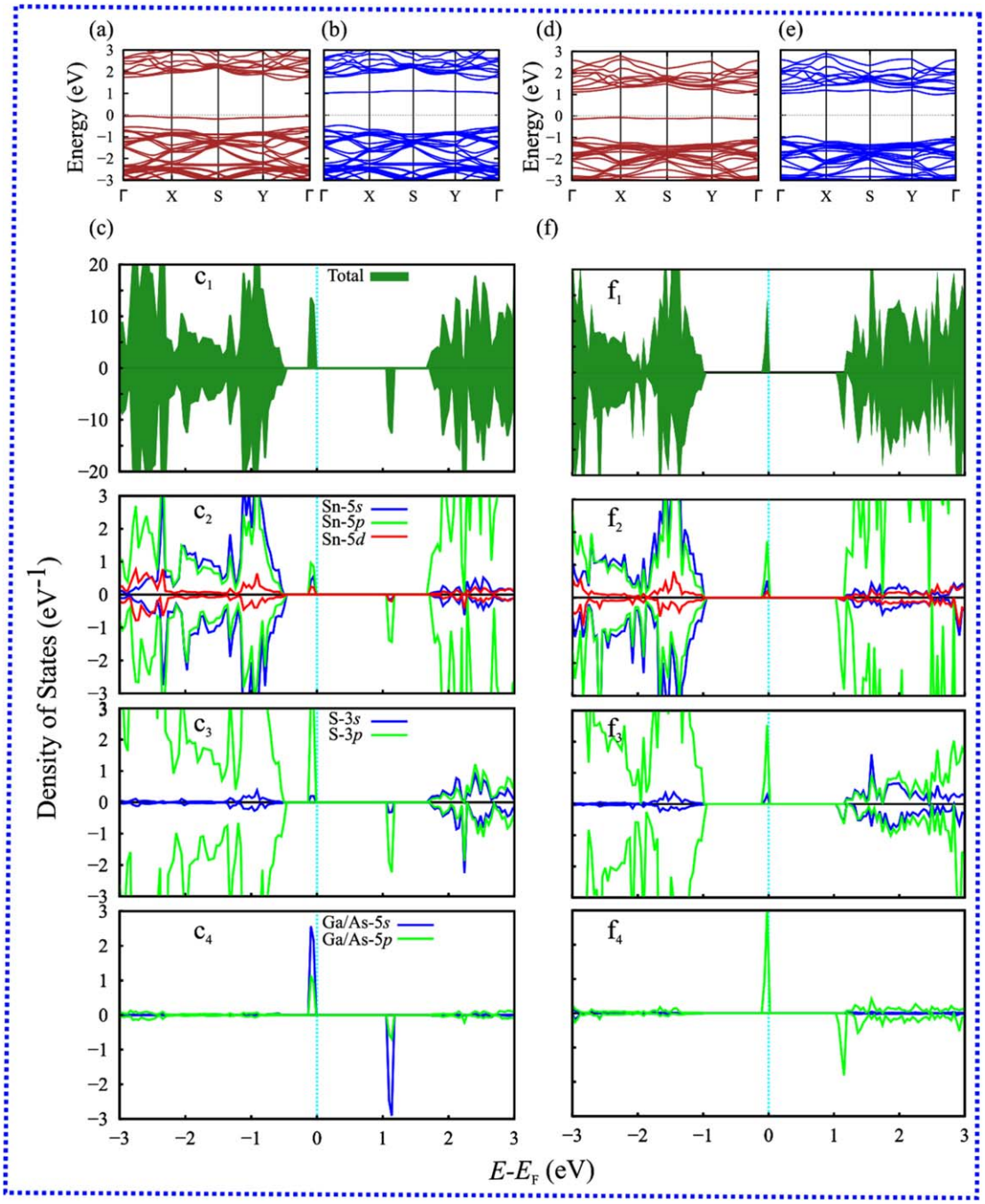

Figure 3. The calculated spin-polarized band structure of monolayer SnS with (a), (b) Ga, (d), (e) As atoms at the Sn-site. The TDOS and PDOS of monolayer SnS with (c (c_1-c_4)) Ga, (f (f_1-f_4)) As atoms at the Sn-site. In the band structure, the brown and blue lines show the spin up and spin down channels.

Mn, Co, and Fe were in high spin state and here in this case the non-magnetic Ga and As atom doping induces spin-polarization in SnS.

The total/local magnatic moments of our studied configurations are given in tables 1, 2. To obtain each atom's magnetic moments, we integrate the spin-polarized density (spherical integration) using VASP default atomic radii. These radii for the atoms Sn, S, Ga, and As are 1.56 Å, 1.16 Å, 1.40 Å, and 1.22 Å, respectively. The local magnetic moments listed in table 2 shows major magnetic moment is localized at the dopant atoms and a smaller contribution can be seen fron the nearby Sn and S atoms. This phenomenon is confirmed by the spin-density that most of the part is localized at both the dopants Ga and As, as shown in figure 4.

The spin-charge density of the doped system is presented in figure 4 to get a clear insight into spin-polarization in doped SnS. It is evident that the dopant atom (Ga and As) induced the spin-polarized magnetic ground. The phenomenon agrees well with the calculated total DOS and PDOS. Also, the dopants Ga/As urges to an acceptor level.

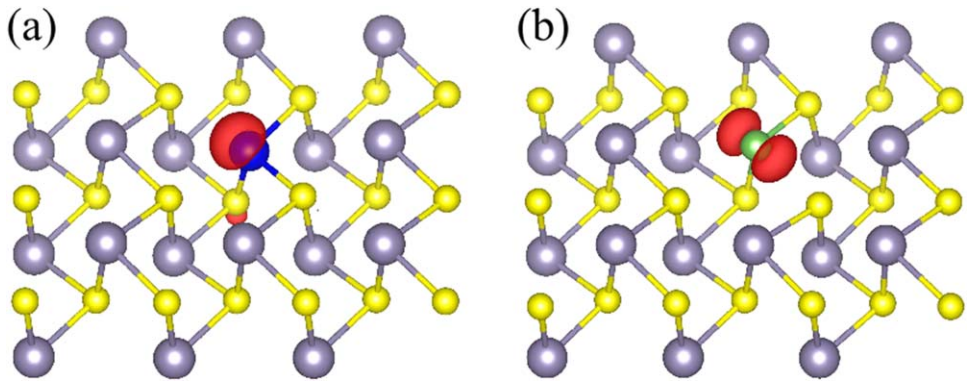

Figure 4. The spin-density difference ($\rho_{(up)} - \rho_{(down)}$) of (a) Ga-, and (b) As doped monolayer SnS. The isosurfaces are set at 3 × 10^{-3} e Å^{-3}.

Table 2. The calculated magnetic moments (μ_{local}) of the dopants Ga/As and the nearby Sn/S atoms to the dopants in monolayer SnS.

Dopant	Ga		As	
μ_{local} (μ_B)	0.31		0.30	
Nearest atoms	Sn	S	Sn	S
μ_{local} (μ_B)	0.01	0.06	0.02	0.03

Furthermore, the FMs and AFMs coupling between the impurity atoms with 5.88% concentration taken into account for the dopants to study its magnatic ground state. For the FM/AFM states, the orientations are set, keeping the spin parallel and antiparallel between the dopant atoms. In general, the magnetic interactions between the two dopants vary with varying the distance between them [18, 48]. For this purpose, we vary the distance between the dopants. We consider different configurations by keeping the two dopants at varying positions in both the same and different Sn-plane. Our analysis exhibits that the dopants that replaced the Sn atom in the same Sn-plane are energetically favorable than the dopants in different Sn-plane. In this study, we consider three different configurations by keeping the two dopants at distances 4.08 Å, 8.16 Å, and 12.24 Å, respectively to compute the interaction between them. The magnetic interaction between the dopants is calculated using the energy difference, $\Delta E = E_{FM} - E_{AFM}$, between the FM and AFM states. The ΔE for the distances 4.08 Å, 8.16 Å, and 12.24 Å, are represented by ΔE_1, ΔE_2, and ΔE_3, respectively. From the table 1, it is observed that for Ga-doped SnS the FM state is the ground state, and the As-doping in SnS favors paramagnetic and AFM states. Note that the ferromagnetism above room temperature is already realized in Mn-doped $SnSe_2$ [53]. We expect that the same approaches might be utilized for realizing spin-polarization in Ga-/As-doped monolayer SnS.

Additionally, we have calculated the magnetic anisotropy of the Ga- and As-doped monolayer SnS. Considering the ground state structure of the Ga- and As-doped systems, we performed a non-collinear calculation with the inclusion of spin–orbit coupling by taking the magnetic axes along [100], [010], and [001] directions. The hard axes are known to be the one with highest energy and the lowest energy direction is said to be an easy axis. The difference in energy between hard and easy axes gives the magneto-crystalline anisotropy energy [41, 54]. For the Ga- and As-doped monolayer SnS, the spin-polarization in *x*-direction, [100], has a lower energy (easy axes) and the y-direction i.e. [010] has the high energy (hard axis). The MAEs ($E_{[010]} - E_{[100]}$) for Ga-/As-doped monolayer SnS are computed to be 0.87 meV, 0.08 meV, respectively. Our calculated MAE is comparable to the doped materials such as phosphorene [54], and 3*d* magnetic nanostructures [54, 55]. Thus, the Ga- and As-doped monolayer SnS endows the possible application at a high temperature.

4. Summar

In summary, we used first-principles calculation to explore the electronic and magnetic properties of Ga-/As-doped monolayer SnS at the Sn-site. We found that both the dopants are energetically favourable in SnS due to larger binding energies. Significant changes in the electronic properties are observed with doping Ga and As atoms in SnS at the Sn-site. Both the dopants changed the semiconductor SnS to the magnetic one. When Ga (As) atom replaces Sn atom, a hole (an unpaired electron) has been induced in the system showing the *p*-type

(n-type) doping. Interestingly, spin-polarization with a magnetic moment of 1.00 μ_B has been induced in both the Ga- and As-doped monolayer SnS. Moreover, the realization of MAE could furnish a way for the promising use of Ga- and As-doped monolayer SnS in 2D photo-electronic and magnetic semiconductor devices.

Acknowledgments

The author (H I El Saeedy) extends his appreciation to the Deanship of Scientific Research at King Khalid University for funding this work through General Research Project Under Grant Number (GRP/158/42).

Data availability statement

The data that support the findings of this study are available upon reasonable request from the authors.

ORCID iDs

Hamid Ullah https://orcid.org/0000-0001-7304-8863
Asad Ali https://orcid.org/0000-0002-8196-8691
N A Noor https://orcid.org/0000-0001-8039-1424
Young-Han Shin https://orcid.org/https://orcid.org/0000-0002-8537-1905

References

[1] Yu W, Zhu Z, Niu C-Y, Li C, Cho J-H and Jia Y 2015 Anomalous doping effect in black phosphorene using first-principles calculations *Phys. Chem. Chem. Phys.* **17** 16351–8
[2] Vogt P, De Padova P, Quaresima C, Avila J, Frantzeskakis E, Asensio M C, Resta A, Ealet B and Le Lay G 2012 Silicene: compelling experimental evidence for graphenelike two-dimensional silicon *Phys. Rev. Lett.* **108** 155501
[3] Xia W, Hu W, Li Z and Yang J 2014 A first-principles study of gas adsorption on germanene *Phys. Chem. Chem. Phys.* **16** 22495–8
[4] Zhu F, Chen W, Xu Y, Gao C, Guan D, Liu C, Qian D, Zhang S-C and Jia J 2015 Epitaxial growth of two-dimensional stanene *Nat. Mater.* **14** 1020–5
[5] Geim A K and Novoselov K S 2007 The rise of graphene *Nat. Mater.* **6** 183–91
[6] Novoselov K S, Geim A K, Morozov S V, Jiang D, Zhang Y, Dubonos S V, Grigorieva I V and Firsov A A 2004 Electric field effect in atomically thin carbon films *Science* **306** 666–9
[7] Rodin A S, Carvalho A and Castro Neto A H 2014 Strain-induced gap modification in black phosphorus *Phys. Rev. Lett.* **112** 176801
[8] Brumme T, Calandra M and Mauri F 2015 First-principles theory of field-effect doping in transition-metal dichalcogenides: structural properties, electronic structure, Hall coefficient, and electrical conductivity *Phys. Rev.* B **91** 155436
[9] Sivek J, Şahin H, Partoens B and Peeters F M 2013 Adsorption and absorption of boron, nitrogen, aluminum, and phosphorus on silicene: stability and electronic and phonon properties *Phys. Rev.* B **87** 085444
[10] Zhang H, Ma Y and Chen Z 2015 Quantum spin hall insulators in strain-modified arsenene *Nanoscale* **7** 19152–9
[11] Zhang S, Yan Z, Li Y, Chen Z and Zeng H 2015 Atomically thin arsenene and antimonene: semimetal–semiconductor and indirect–direct band-gap transitions *Angew. Chem. Int. Ed.* **54** 3112–5
[12] Zhang S, Xie M, Li F, Yan Z, Li Y, Kan E, Liu W, Chen Z and Zeng H 2016 Semiconducting group 15 monolayers: a broad range of band gaps and high carrier mobilities *Angew. Chem.* **128** 1698–701
[13] Zhu Z, Guan J, Liu D and Tománek D 2015 Designing isoelectronic counterparts to layered group V semiconductors *ACS Nano* **9** 8284–90
[14] Parenteau M and Carlone C 1990 Influence of temperature and pressure on the electronic transitions in SnS and SnSe semiconductors *Phys. Rev.* B **41** 5227–34
[15] Choi J, Jin J, Jung I G, Kim J M, Kim H J and Son S U 2011 $SnSe_2$ nanoplate–graphene composites as anode materials for lithium ion batteries *Chem. Commun.* **47** 5241–3
[16] Qu H, Guo S, Zhou W and Zhang S 2021 Uncovering the Anisotropic Electronic Structure of 2D Group VA-VA Monolayers for QuantumTransport *IEEE Electron Device Lett.* **42** 66-9
[17] Nassary M M 2005 Temperature dependence of the electrical conductivity, Hall effect and thermoelectric power of SnS single crystals *J. Alloys Compd.* **398** 21–5
[18] Ullah H, Noor-A-Alam M, Kim H J and Shin Y-H 2018 Influences of vacancy and doping on electronic and magnetic properties of monolayer SnS *J. Appl. Phys.* **124** 065102
[19] Ettema A R H F, de Groot R A, Haas C and Turner T S 1992 Electronic structure of SnS deduced from photoelectron spectra and band-structure calculations *Phys. Rev.* B **46** 7363–73
[20] Banai R E, Horn M W and Brownson J R S 2016 A review of tin (II) monosulfide and its potential as a photovoltaic absorber *Sol. Energy Mater. Sol. Cells* **150** 112–29
[21] Burton L A and Walsh A 2012 Phase stability of the earth-abundant tin sulfides SnS, SnS_2, and Sn_2S_3 *J. Phys. Chem.* C **116** 24262–7
[22] Reddy N K, Devika M and Gopal E S R 2015 Review on tin (II) sulfide (SnS) material: synthesis, properties, and applications *Crit. Rev. Solid State Mater. Sci.* **40** 359–98
[23] Wu M and Zeng X C 2016 Intrinsic ferroelasticity and/or multiferroicity in two-dimensional phosphorene and phosphorene analogues *Nano Lett.* **16** 3236–41
[24] Hanakata P Z, Carvalho A, Campbell D K and Park H S 2016 Polarization and valley switching in monolayer group-IV monochalcogenides *Phys. Rev.* B **94** 035304

[25] Fei R, Li W, Li J and Yang L 2015 Giant piezoelectricity of monolayer group IV monochalcogenides: Snse, Sns, Gese, and Ges *Appl. Phys. Lett.* **107** 173104
[26] Hu F F, Tang H Y, Tan C J, Ye H Y, Chen X P and Zhang G Q 2017 Nitrogen dioxide gas sensor based on monolayer SnS: a first-principle study *IEEE Electron Device Lett.* **38** 983–6
[27] Yang Z, Du G, Meng Q, Guo Z, Yu X, Chen Z, Guo T and Zeng R 2011 Dispersion of SnO_2 nanocrystals on TiO_2(B) nanowires as anode material for lithium ion battery applications *RSC Adv.* **1** 1834–40
[28] Xiao G, Wang Y, Ning J, Wei Y, Liu B, Yu W W, Zou G and Zou B 2013 Recent advances in IV–VI semiconductor nanocrystals: synthesis, mechanism, and applications *RSC Adv.* **3** 8104–30
[29] Noguchi H, Setiyadi A, Tanamura H, Nagatomo T and Omoto O 1994 Characterization of vacuum-evaporated tin sulfide film for solar cell materials *Sol. Energy Mater. Sol. Cells* **35** 325–31
[30] Parveen B, Hassan M, Atiq S, Riaz S, Naseem S and Toseef M A 2017 Structural and dielectric study of nano-crystalline single phase Sn1−xNixS (xNi=0–10%) showing room temperature ferromagnetism *Progress in Natural Science: Materials International* **27** 303–10
[31] Yang Y L, Cheng S Y and Lai S L 2009 Effect of Ag doping on structural, optical and electrical properties of SnS:Ag thin films prepared by pulse electroposition *Advanced Materials Research* **60–61** 105–9
[32] Chaki S H, Chaudhary M D and Deshpande M P 2015 Effect of indium and antimony doping in SnS single crystals *Mater. Res. Bull.* **63** 173–80
[33] Chaki S H, Deshpande M P, Trivedi D P, Tailor J P, Chaudhary M D and Mahato K 2013 Wet chemical synthesis and characterization of SnS_2 nanoparticles *Appl. Nanosci.* **3** 189–95
[34] Kohn W and Sham L J 1965 Self-consistent equations including exchange and correlation effects *Phys. Rev.* **140** A1133–8
[35] Perdew J P, Burke K and Ernzerhof M 1996 Generalized gradient approximation made simple *Phys. Rev. Lett.* **77** 3865–8
[36] Perdew J P, Burke K and Ernzerhof M 1997 Generalized gradient approximation made simple [Phys. Rev. Lett. 77, 3865 (1996)] *Phys. Rev. Lett.* **78** 1396–1396
[37] Kresse G and Furthmüller J 1996 Efficient iterative schemes for *ab initio* total-energy calculations using a plane-wave basis set *Phys. Rev.* B **54** 11169–86
[38] Heyd J, Scuseria G E and Ernzerhof M 2003 Hybrid functionals based on a screened Coulomb potential *J. Chem. Phys.* **118** 8207–15
[39] Heyd J, Scuseria G E and Ernzerhof M 2006 Erratum: 'Hybrid functionals based on a screened Coulomb potential' [J. Chem. Phys. 118, 8207 (2003)] *The Journal of Chemical Physics* **124** 219906
[40] Hobbs D, Kresse G and Hafner J 2000 Fully unconstrained noncollinear magnetism within the projector augmented-wave method *Phys. Rev.* B **62** 11556–70
[41] Rocquefelte X, Schwarz K, Blaha P, Kumar S and van den Brink J 2013 Room-temperature spin-spiral multiferroicity in high-pressure cupric oxide *Nat. Commun.* **4** 2511
[42] Cheng Y C, Zhu Z Y, Mi W B, Guo Z B and Schwingenschlögl U 2013 Prediction of two-dimensional diluted magnetic semiconductors: doped monolayer MoS_2 systems *Phys. Rev.* B **87** 100401
[43] Gomes L C and Carvalho A 2015 Phosphorene analogues: isoelectronic two-dimensional group-IV monochalcogenides with orthorhombic structure *Phys. Rev.* B **92** 085406
[44] Hou W, Mi H, Peng R, Peng S, Zeng W and Zhou Q 2021 First-principle insight into Ga-doped MoS_2 for sensing SO_2, SOF_2 and SO_2F_2 *Nanomaterials (Basel)* **11** 314
[45] Liu L, Ji Y, Liu Y and Liu L 2019 First Principle Studies on the Ga and As Doping of Germanane Monolayer *Journal of Applied Mathematics and Physics* **7** 46–54
[46] Chappert C, Fert A and Dau F N V 2007 The emergence of spin electronics in data storage *Nat. Mater.* **6** 813
[47] Seminovski Y, Palacios P and Wahnón P 2014 Analysis of SnS_2 hyperdoped with V proposed as efficient absorber material *J. Phys. Condens. Matter* **26** 395501
[48] Ullah H, Noor-A-Alam M and Shin Y-H 2020 Vacancy- and doping-dependent electronic and magnetic properties of monolayer SnS_2 *J. Am. Ceram. Soc.* **103** 391–402
[49] Wang Y, Li S and Yi J 2016 Electronic and magnetic properties of Co doped MoS_2 monolayer *Sci. Rep.* **6** 24153
[50] Chen H, Li Y, Huang L and Li J 2015 Influential electronic and magnetic properties of the gallium sulfide monolayer by substitutional doping *J. Phys. Chem.* C **119** 29148–56
[51] Fan X-L, An Y-R and Guo W-J 2016 Ferromagnetism in transitional metal-doped MoS_2 monolayer *Nanoscale Res. Lett.* **11** 154
[52] Xiao W-Z, Xiao G, Rong Q-Y, Chen Q and Wang L-L 2017 Electronic and magnetic properties of SnS_2 monolayer doped with 4d transition metals *J. Magn. Magn. Mater.* **438** 152–62
[53] Dong S *et al* 2016 Room temperature weak ferromagnetism in $Sn_{1-x}Mn_xSe_2$ 2D films grown by molecular beam epitaxy *APL Materials* **4** 032601
[54] Khan I and Hong J 2016 Magnetic properties of transition metal Mn, Fe and Co dimers on monolayer phosphorene *Nanotechnology* **27** 385701
[55] Hu J, Wang P, Zhao J and Wu R 2018 Engineering magnetic anisotropy in two-dimensional magnetic materials *Adv. Phys.* X **3** 1432415